*COVID*

MDPI

*Article*

# A Reciprocal Cross-Reactivity between Monoclonal Antibodies to SARS-CoV-2 Spike Glycoprotein S1 and Human CXCR2—An Implication of a Viral Mimic of Human CXCR2

**Tatsushi Mizutani**

Department of Pediatrics, Daiyukai General Hospital, Daiyukai Health System, Ichinomiya, Aichi 491-8551, Japan; mizutani.t1@med.nagoya-u.ac.jp

**Abstract:** Some viruses contain mimics of host chemokine receptors that influence host immunity; however, such viral mimics have not yet been reported for severe acute respiratory syndrome coronavirus 2 (SARS-CoV-2). In this study, I focused on C-X-C motif chemokine receptor 2 (CXCR2) as a candidate chemokine receptor exploited by SARS-CoV-2. Similarities between the extracellular domain (ECD) of human CXCR2 and the SARS-CoV-2 spike glycoprotein S1 (CoV2S1) were investigated. Flow cytometric analysis of healthy donor-derived peripheral leukocytes was performed to examine the cross-reactivity between specific monoclonal antibodies against these two proteins. The results showed that CR3022, a monoclonal antibody to the receptor binding domain of CoV2S1, recognized the CXCR2 ECD, and a murine monoclonal antibody to human CXCR2 recognized recombinant CoV2S1. This reciprocal cross-reactivity suggests that CoV2S1 harbors a mimic of the CXCR2 ECD.

**Keywords:** SARS-CoV-2 spike glycoprotein S1; viral chemokine receptor; CXCR2; IL8; CR3022



**Citation:** Mizutani, T. A Reciprocal Cross-Reactivity between Monoclonal Antibodies to SARS-CoV-2 Spike Glycoprotein S1 and Human CXCR2—An Implication of a Viral Mimic of Human CXCR2. *COVID* **2022**, *2*, 569–577. https://doi.org/10.3390/covid2050042

Academic Editor: Francesco Caruso

Received: 12 April 2022
Accepted: 1 May 2022
Published: 2 May 2022



## 1. Introduction

Some viruses reportedly evade host immunity by acquiring mimics of host chemokine receptors during the genetic process of virus–host coevolution [1]. Because chemokine receptors possess multiple chemokines as their own cognate ligands [2], such viral mimics can lead to global alterations in host chemokine-mediated functions, such as leukocyte chemotaxis, angiogenesis, and neuronal maintenance.

The severity of severe acute respiratory syndrome coronavirus 2 (SARS-CoV-2) pneumonia has been associated with the overexpression of ligands that activate the C-X-C motif chemokine receptor 2 (CXCR2) pathway in the nasopharynx [3]. The serum levels of CXCL2 and CXCL8 (interleukin (IL)8), both of which are chemokine ligands for CXCR2, are also significantly elevated in the early phase of infection [4]. Given that the CXCR2-mediated axis plays an important role in controlling peripheral granulocyte migration, extravasation, and endothelial homeostasis [5], prolonged dysregulation of this axis may induce aberrant recruitment of activated granulocytes and embolic pathology, as observed in advanced cases of SARS-CoV-2 infection [6–9]. As coronaviruses possess an exceptionally high potential for genetic recombination ability relative to other RNA viruses [10,11], SARS-CoV-2 may have implemented host gene fragments into its own genome during evolution [12]. Thus, SARS-CoV-2 may harbor a mimic of human CXCR2 that induces pathological consequences by altering the CXCR2-mediated axis in peripheral granulocytes.

CXCR2 is a chemokine G-protein-coupled receptor (GPCR). Its extracellular domain (ECD) is composed of an N-terminal domain (NTD) and three extracellular loops (I–III) [5]. CXCR2 can recognize not only IL8 but also a broader variety of C-X-C chemokines through discontinuous amino acid sequences in the NTD [13–15]. The IL8-binding amino acid sequences of the CXCR2 NTD wrap around the IL8 globular core mainly through hydrophobic interactions to form an IL8–CXCR2-NTD complex. This complex attaches to

the CXCR2 extracellular loops by bending and positioning through a disulfide bond between the NTD and extracellular loop III, leading to the activation of intracellular signaling pathways for granulocyte chemotactic migration [5,14,16].

IL8 binding to the CXCR2 NTD induces internalization of the IL8–CXCR2 complex to desensitize the receptor in an IL8 concentration-dependent manner. This binding also contributes to the termination of granulocyte chemotactic migration at the inflammatory site, where the local IL8 concentration is the highest [17,18]. Therefore, aberrant recruitment of activated peripheral granulocytes during SARS-CoV-2 infection may be a secondary event due to the perturbed formation of the CXCR2 chemokine-concentration gradient at the site of viral infection.

To elucidate the accumulation of activated granulocytes observed in SARS-CoV-2 infection, I investigated whether it is possible that SARS-CoV-2 harbors a mimic of the ECD in human CXCR2. To identify the location of such a mimic, the SARS-CoV-2 spike glycoprotein S1 domain (CoV2S1) of the original Wuhan-Hu strain was examined.

## 2. Materials and Methods

This study was performed from July to November in 2021.

### *2.1. Study 1 Flow Cytometric Analysis for Samples without Recombinant CoV2S1 (rCoV2S1)*

#### 2.1.1. Preparation of Peripheral Leukocytes

Peripheral blood samples were collected from two healthy adult donors (see Supplementary Table S1 for healthy donor information). Whole blood (2 mL) in a collecting tube coated with EDTA-2K (453533; Sekisui Medical, Tokyo, Japan) was centrifuged at 400× *g* for 10 min. After plasma removal, the remaining sample was mixed with 5 mL of 1× red blood cell (RBC) lysis buffer diluted from a 10× stock (420301; BioLegend, San Diego, CA, USA) and incubated at room temperature for 10 min. To stop the lysis reaction, 30 mL of 1× phosphate-buffered saline (PBS) was added to the mixture, which was then centrifuged at 400× *g* for 10 min, and the supernatant was aspirated. RBC lysis was repeated twice. The pellet was resuspended in 1000 µL of flow cytometry buffer (FACS buffer, 1× PBS containing 1% bovine serum albumin and 0.2% sodium azide). Approximately 140 µL aliquots of the suspension containing $10^5$–$10^6$ leukocytes were transferred into FACS tubes (Falcon 352235; Corning Inc., Corning, NY, USA). The cells were washed with 1 mL of FACS buffer and centrifuged at 400× *g* for 5 min, and the supernatant was discarded.

#### 2.1.2. Reagents

CR3022 (273074; Abcam, Cambridge, UK) was used as a rabbit monoclonal antibody to CoV2S1. A monoclonal rabbit IgG (3900S; Cell Signaling Technology, Danvers, MA, USA) was used as an isotype control for CR3022. Donkey polyclonal Alexa Fluor 647-conjugated anti-rabbit IgG (AF 647/anti-rabbit IgG; 406414; BioLegend) was used to detect CR3022 and the isotype control. A human Fc block (564220; BD Biosciences, Franklin Lakes, NJ, USA) was used to avoid nonspecific Fc receptor-mediated antibody binding to leukocytes. Murine monoclonal PE/anti-human CD182 (CXCR2; 320705; BioLegend), murine monoclonal FITC/anti-human CD181 (CXCR1; 320605; BioLegend), and murine monoclonal BV421/anti-human CD66b (305111; BioLegend) were used to detect granulocytes. The threshold for detecting flow cytometry signals was determined through in-house titration as listed in Supplementary Table S2.

#### 2.1.3. Cell Staining and Flow Cytometric Analysis

Cells in the FACS tube were incubated with Fc block, which was diluted with 30 µL of FACS buffer for 10 min on ice. Subsequently, 40 µL of FACS buffer containing a mixture of primary antibodies against murine monoclonal PE/anti-human CXCR2, murine monoclonal FITC/anti-human CXCR1, murine monoclonal BV421/anti-human CD66b, and rabbit monoclonal CR3022 was incubated for 20 min on ice. The same dose of isotype IgG was incubated instead of CR3022 as a negative control. The cells were washed once

with FACS buffer, resuspended in FACS buffer containing AF 647/anti-rabbit IgG as the secondary antibody against CR3022, and incubated for 20 min on ice. The cells were then washed twice with FACS buffer, and 1 µL of 7-AAD (559925; BD Biosciences) was added to exclude nonviable cells. The fluorescence intensity of the sample was measured using an FACS Aria II (BD Biosciences). The number of electrical events for the measurements per sample was set at 30,000 in the live-cell population. The data were analyzed using FlowJo (v10.0; FlowJo LLC, Ashland, OR, USA).

### *2.2. Study 2 Flow Cytometric Analysis for Samples with rCoV2S1*

rCoV2S1 (273068; Abcam, Cambridge, UK) contains an amino acid sequence that covers Val16 to Arg685 of the original Wuhan-Hu strain. rCoV2S1 is cytometrically detectable by incubation with a fluorochrome-conjugated anti-spike S1 antibody in cells overexpressing angiotensin-converting enzyme 2 (ACE2) [19]. The experimental procedures in Study 1 were repeated by adding rCoV2S1 to a mixture of primary antibodies.

The protocols of studies 1 and 2 were repeated three times on different days to confirm the within-subject repeatability of the 1st subject. To confirm the between-subject repeatability, the protocols of studies 1 and 2 were performed for the 2nd subject.

## 3. Results

The same results were obtained in studies 1 and 2 three times for the 1st and 2nd subjects.

### *3.1. Study 1*

#### Monoclonal Anti-SARS-CoV-2 Spike S1 Antibody (CR3022) Recognizes the ECD of Human CXCR2

The similarities between the ECD of human CXCR2 and CoV2S1 were evaluated using multicolor flow cytometric analysis of fresh leukocytes obtained from two healthy donors. Whether CR3022, a monoclonal anti-SARS-CoV-2 spike S1 antibody against non-ACE2-binding sites in the receptor binding domain of CoV2S1 [20], cross-reacts with the ECD of human CXCR2 was examined. Murine monoclonal antibodies against the ECD of human CXCR2 and CXCR1, which is homologous to human CXCR2, were used. A murine monoclonal antibody against CD66b, a specific surface marker of the granulocytic lineage, was also used. The entire leukocyte population of interest was defined using the gating strategy shown in Supplementary Figure S1. The intensity of CR3022 (red) showed a significant rightward shift compared with that of the negative control (blue), indicating that CR3022 recognized granulocytes. However, in the non-granulocyte population (Figure 1a–c, *), the intensity of CR3022 completely overlapped with that of the negative control, indicating that CR3022 did not recognize the non-granulocyte population. The signal intensity of CR3022 in the granulocyte population was positively correlated with the anti-human CXCR2 antibody (Figure 1a). In contrast, the cross-reactivity of CR3022 with the granulocyte population did not correlate with CXCR1 and CD66b (Figure 1b,c). These results suggest that CR3022 recognizes the ECD of human CXCR2 based on the observed specific cross-reactivity of CR3022 against the ECD of human CXCR2.

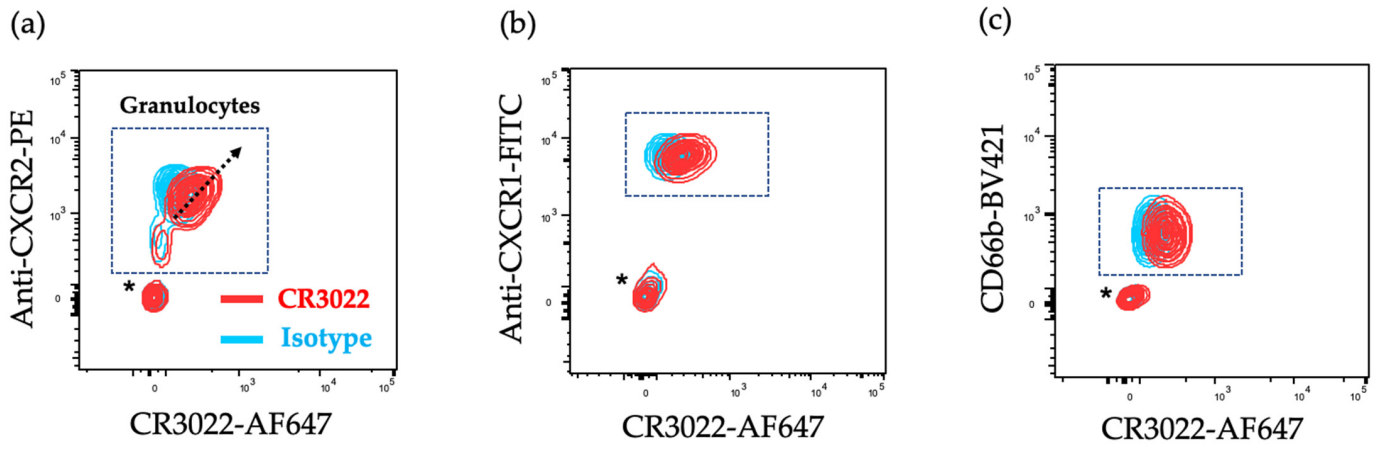


**Figure 1.** Representative results of flow cytometric analysis for samples without recombinant CoV2S1 (rCoV2S1). The dashed-line rectangle shows a biexponential contour plot of the signal intensity of the fluorochrome conjugated with antibodies on granulocytes (see Supplementary Figure S1 for the definition of the granulocyte population). * shows non-granulocyte population. CR3022-Alexa Fluor (AF)647 indicates the signal intensity of AF647 conjugated to CR3022. Anti-CXCR2-phycoerythrin (PE) refers to the signal intensity of PE conjugated to the anti-CXCR2 antibody. Anti-CXCR1-fluorescein isothiocyanate (FITC) indicates the signal intensity of FITC conjugated to the anti-CXCR1 antibody. Anti-CD66b-Brilliant Violet (BV)421 indicates the signal intensity of BV421 conjugated with the anti-CD66b antibody. (**a**–**c**) The red population in the rectangle shows granulocytes with CXCR2 vs. CR3022, CXCR1 vs. CR3022, and CD66b vs. CR3022, respectively (see details in theSection 2). CR3022 was replaced with rabbit monoclonal IgG as a negative control and expressed and overlaid in blue. The signal intensity of CR3022-AF647 was significantly correlated with the anti-CXCR2-PE signal in the granulocyte population (**a**, dashed-line arrow); however, there was no significant correlation between CR3022 and anti-CXCR1 or anti-CD66b ((**b**,**c**), respectively). The experiment was repeated three times. Dot plots in (**a**–**c**) are shown in Supplementary Figure S2.

### *3.2. Study 2*

### Monoclonal Anti-ECD of the Human CXCR2 Antibody Recognizes rCoV2S1

The cross-reactivity of the anti-human CXCR2 antibody against CoV2S1 was examined by incubating leukocytes with a mixture of primary antibodies and rCoV2S1. rCoV2S1 is not directly detectable using flow cytometry; thus, cross-reactivity was estimated indirectly based on the reduction in the signal intensity of the anti-human CXCR2 antibody in the leukocyte population caused by the competitive effect of rCoV2S1. Different concentrations of rCoV2S1 (0, 0.5, 1.5, and 3 μg per sample) were prepared to examine the dose-dependency of the reduction caused by anti-human CXCR2 antibody binding to rCoV2S1.

A competitive effect of rCoV2S1 on CR3022 in the granulocyte population due to the binding of CR3022 to rCoV2S1 was clearly observed at rCoV2S1 concentrations of 0–3 μg (Figure 2a). The signal intensity of anti-human CXCR2 antibodies in the same granulocyte population decreased with increasing concentrations of rCoV2S1 (Figure 2b). This result indicates that rCoV2S1 competed with the anti-human CXCR2 antibody, suggesting cross-reactivity of the anti-human CXCR2 antibody with rCoV2S1. These results, along with those described in Section 3.1, showed that CR3022, a specific monoclonal antibody against CoV2S1 and rCoV2S1, recognized the ECD of human CXCR2. Additionally, a murine monoclonal antibody against the ECD of human CXCR2 recognized rCoV2S1. This reciprocal cross-reactivity suggests that CoV2S1 harbors a mimic of the ECD of human CXCR2.

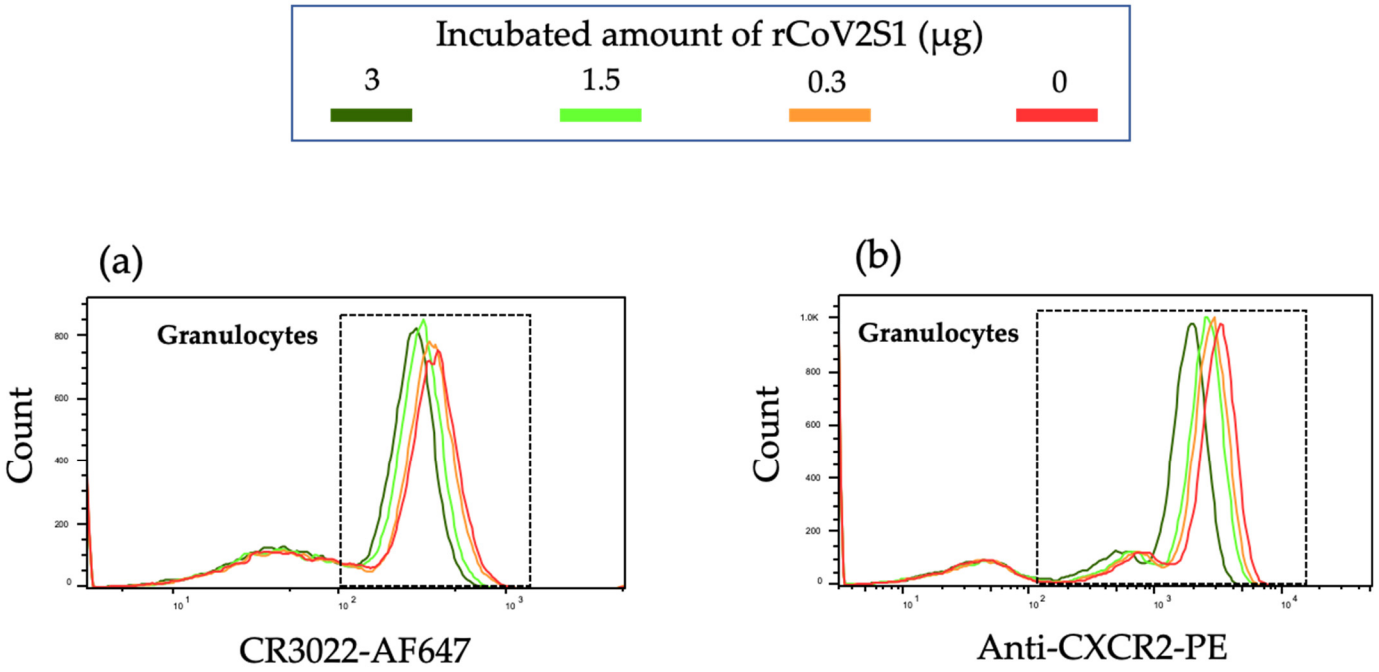


**Figure 2.** Representative results of flow cytometric analysis for samples with rCoV2S1. Flow cytometry histograms of the whole leukocyte population co-incubated with rCoV2S1 at different concentrations. The *Y*-axis shows the cell count for the leukocyte population, and the *X*-axis shows the logarithmic signal intensity of fluorochromes conjugated with antibodies. The dashed-line rectangle indicates the granulocyte population. Each profile at rCoV2S1 (0, 0.3, 1.5, or 3.0 μg) is highlighted in red, orange, light-green, and dark-green, respectively. (**a**) The signal intensity of AF647-conjugated CR3022 in the granulocyte population decreased as the concentration of rCoV2S1 increased. (**b**) The signal intensity of PE-conjugated anti-human CXCR2 in the same granulocyte population decreased as the concentration of rCoV2S1 increased. The experiment was repeated three times.

## 4. Discussion

This study showed that CoV2S1 may harbor a viral mimic of human CXCR2, which is the IL8 receptor. Increased levels of IL8 reportedly correlate with the severity of SARS-CoV-2 infection [21,22]. Viruses and viral proteins can upregulate *IL8* transcription, which is translated and secreted by endothelial cells, epithelial cells, and peripheral leukocytes [23]. IL8 in the bloodstream is captured by upregulated heparan sulfate on endothelial cells at the infection site to form an IL8 concentration gradient and attract peripheral granulocytes to undergo chemotactic migration and extravasation [24]. The chemotactic migration of peripheral granulocytes is regulated by CXCR2 [25]. Rose et al. [17] showed that CXCR2 signaling driving granulocyte migration is counter-regulated by receptor desensitization following receptor-IL8 complex internalization in an IL8 concentration-dependent manner. They suggested that receptor endocytosis acts as a terminal stop signal when granulocytes reach the infection site, where the IL8 concentration is the highest.

Viral mimics of human GPCR chemokine receptors are exploited by some large DNA viruses to escape host immunity [1]. One important example is the viral mimic of human C-$X_3$-C and C-C chemokine receptors, which is referred to as US28 and encoded by human cytomegalovirus. US28 can bind to a broad variety of chemokines, including $CX_3CL1$, and ligands for C-C chemokine receptor 5 (CCR5), such as CCL5 (also known as RANTES) [26]. Human CCR5 plays an important role in host defense mechanisms through T cell migration and adaptive immune functions [27,28]. Bodaghi et al. [29] reported that US28 sequesters C-C chemokines such as RANTES in virus-infected cells, and that the sequestration of host RANTES by the viral mimic leads to a decrease in the extracellular RANTES concentration. Additionally, Billstrom et al. [30] demonstrated

that RANTES concentration is decreased by internalization of the membrane-bound RANTES–US28 complex in virus-infected cells and suggested that CCR5-mediated chemotactic activity is perturbed in host cells. The structural similarities between human proteins and SARS-CoV-2 have been studied using computational approaches [31,32]. I hypothesized that a viral mimic of human CXCR2 is embedded in CoV2S1. The flowcytometric analysis using healthy donor-derived leukocytes revealed reciprocal cross-reactivity between specific monoclonal antibodies against the ECD of human CXCR2 and rCoV2S1 (Figures 1a and 2b), suggesting similarities between the ECD of human CXCR2 and CoV2S1.

CR3022, a monoclonal antibody to the receptor binding domain of CoV2S1 [20], recognizes the ECD of human CXCR2 (Figure 1a). A monoclonal anti-NTD of the human CXCR2 antibody (abN48) reportedly induces receptor internalization after binding to the NTD of human CXCR2 [15]. As CR3022 cross-reacts with the ECD of CXCR2, human antibodies produced during CoV2 infection may recognize this domain, leading to antibody-dependent desensitization. Moreover, anti-CoV2S1 antibodies that recognize the human CXCR2 ECD may cause antibody-dependent cytotoxicity. A previous study suggested that CoV2S1 activates autoreactive T cells by cross-reacting with the T cell receptor (TCR) [33]. Cheng et al. [34] demonstrated that this TCR cross-reactivity is induced through a similar motif as bacterial superantigen, which is located adjacent to the C-terminus of CoV2S1. In the present study, CoV2S1 was found to be similar to human CXCR2. This finding suggests that molecular mimicry, which is defined as a viral mimic of host protein [35], contributes to the TCR cross-reactivity of CoV2S1. In some viruses, molecular mimicry in a viral protein reportedly mediates autoimmune reactions related to viral infection and vaccination [35,36]. It is of clinical significance to elucidate whether the human CXCR2 mimic leads to autoimmune pathologies, as observed in the case of SARS-CoV-2 [37,38].

The flowcytometric analysis showed that a murine monoclonal anti-ECD of human CXCR2 antibody recognized rCoV2S1 (Figure 2b), indicating that CoV2S1 harbors a mimic of the CXCR2 ECD. Notably, epitopes of murine monoclonal antibodies to human CXCR2 closely overlap with the IL8-binding sites of the CXCR2 NTD [15,39–41]. Thus, CoV2S1 may attract IL8 through the mimic of the CXCR2 ECD and induce its unavailability around granulocytes.

Because membrane-bound IL8 in endothelial cells plays a major role in forming a local IL8 concentration gradient [24], its unavailability may affect CXCR2-mediated chemotactic granulocyte migration. A previous study reported that CXCR2 signaling is counter-regulated through receptor desensitization in an IL8-concentration-dependent manner [17]. This counter-regulation is important for terminating the chemotactic migration of granulocytes at the infection site, where the local IL8 concentration is the highest [17]. If the mimic of CXCR2 in CoV2S1 attracts IL8 and contributes to its unavailability, the local concentration gradient of IL8 at the infection site may be perturbed.

This study had some limitations. First, only the rCoV2S1 of the Wuhan-Hu strain was used in this study. Second, the binding affinity of rCoV2S1 to IL8 and chemotactic ability were not measured. Third, structural analyses were not performed. Finally, a small number of healthy donors was examined.

## 5. Conclusions

A reciprocal cross-reactivity occurs between monoclonal antibodies to SARS-CoV-2 spike glycoprotein S1 and human CXCR2. Further studies of the viral characteristics may contribute to the development of new therapeutic compounds.

**Supplementary Materials:** The following information can be downloaded at https://www.mdpi.com/article/10.3390/covid2050042/s1: Figure S1: Gating strategy to define the leukocyte population of interest; Figure S2: Representative results of flow cytometric analysis for samples without recombinant CoV2S1 (rCoV2S1) presented as a dot plot; Table S1: Healthy donor information; Table S2: Overview of reagents used for flow cytometric analysis. Ref. [42] is cited in Supplementary Materials.

**Funding:** This study was supported by a donation for promoting academic research from Daiyukai Health System to the Department of Public Health at Nagoya City University (funding number KIFUK20044).

**Institutional Review Board Statement:** This study was conducted in accordance with the Declaration of Helsinki and approved by the ethics board of the Daiyukai Health System (approval number 2020-020) for studies involving humans.

**Informed Consent Statement:** Written informed consent was obtained from all examinees who donated peripheral blood for flow cytometric analysis.

**Data Availability Statement:** Raw FACS data are available in a publicly accessible repository. The representative data presented in this study are openly available in FigShare at 10.6084/m9.figshare.19337018 (on 12 April 2022).

**Acknowledgments:** I would like to thank Mitsushi Okazawa for his critical discussion and comments on this study. I also thank Sadao Suzuki for allowing use of the core laboratory at Nagoya City University to conduct experiments. I also greatly appreciate the technical support with the FACS Aria II in the laboratory. Finally, I deeply appreciate Shinichi Ito, the president of the Daiyukai Health System, for encouraging me to perform this study.

**Conflicts of Interest:** The author declares no conflict of interest.

## References

1. Alcami, A. Viral Mimicry of Cytokines, Chemokines and Their Receptors. *Nat. Rev. Immunol.* **2003**, *3*, 36–50. [CrossRef] [PubMed]
2. Zlotnik, A.; Yoshie, O. The Chemokine Superfamily Revisited. *Immunity* **2012**, *36*, 705–716. [CrossRef]
3. Rodriguez, C.; de Prost, N.; Fourati, S.; Lamoureux, C.; Gricourt, G.; N'debi, M.; Canoui-Poitrine, F.; Désveaux, I.; Picard, O.; Demontant, V.; et al. Viral Genomic, Metagenomic and Human Transcriptomic Characterization and Prediction of the Clinical Forms of COVID-19. *PLoS Pathog.* **2021**, *17*, e1009416. [CrossRef] [PubMed]
4. Blanco-Melo, D.; Nilsson-Payant, B.E.; Liu, W.-C.; Uhl, S.; Hoagland, D.; Møller, R.; Jordan, T.X.; Oishi, K.; Panis, M.; Sachs, D.; et al. Imbalanced Host Response to SARS-CoV-2 Drives Development of COVID-19. *Cell* **2020**, *181*, 1036–1045.e9. [CrossRef] [PubMed]
5. Rajarathnam, K.; Schnoor, M.; Richardson, R.M.; Rajagopal, S. How Do Chemokines Navigate Neutrophils to the Target Site: Dissecting the Structural Mechanisms and Signaling Pathways. *Cell Signal.* **2018**, *54*, 69–80. [CrossRef] [PubMed]
6. Ackermann, M.; Verleden, S.E.; Kuehnel, M.; Haverich, A.; Welte, T.; Laenger, F.; Vanstapel, A.; Werlein, C.; Stark, H.; Tzankov, A.; et al. Pulmonary Vascular Endothelialitis, Thrombosis, and Angiogenesis in Covid-19. *N. Engl. J. Med.* **2020**, *383*, 120–128. [CrossRef] [PubMed]
7. Ackermann, M.; Anders, H.-J.; Bilyy, R.; Bowlin, G.L.; Daniel, C.; Lorenzo, R.D.; Egeblad, M.; Henneck, T.; Hidalgo, A.; Hoffmann, M.; et al. Patients with COVID-19: In the Dark-NETs of Neutrophils. *Cell Death Differ.* **2021**, 1–15. [CrossRef]
8. Bonaventura, A.; Vecchié, A.; Dagna, L.; Martinod, K.; Dixon, D.L.; Tassell, B.W.V.; Dentali, F.; Montecucco, F.; Massberg, S.; Levi, M.; et al. Endothelial Dysfunction and Immunothrombosis as Key Pathogenic Mechanisms in COVID-19. *Nat. Rev. Immunol.* **2021**, *21*, 319–329. [CrossRef]
9. Morrissey, S.M.; Geller, A.E.; Hu, X.; Tieri, D.; Ding, C.; Klaes, C.K.; Cooke, E.A.; Woeste, M.R.; Martin, Z.C.; Chen, O.; et al. A Specific Low-Density Neutrophil Population Correlates with Hypercoagulation and Disease Severity in Hospitalized COVID-19 Patients. *JCI Insight* **2021**, *6*, e148435. [CrossRef]
10. Lai, M.M.C. Recombination in Large RNA Viruses: Coronaviruses. *Semin. Virol.* **1996**, *7*, 381–388. [CrossRef]
11. Rehman, S.U.; Shafique, L.; Ihsan, A.; Liu, Q. Evolutionary Trajectory for the Emergence of Novel Coronavirus SARS-CoV-2. *Pathogens* **2020**, *9*, 240. [CrossRef] [PubMed]
12. Li, F. Structure, Function, and Evolution of Coronavirus Spike Proteins. *Ann. Rev. Virol.* **2016**, *3*, 237–261. [CrossRef]
13. Katancik, J.A.; Sharma, A.; Nardin, E. De Interleukin 8, Neutrophil-Activating Peptide-2 and GRO-Alpha Bind to and Elicit Cell Activation via Specific and Different Amino Acid Residues of CXCR2. *Cytokine* **2000**, *12*, 1480–1488. [CrossRef] [PubMed]
14. Liu, K.; Wu, L.; Yuan, S.; Wu, M.; Xu, Y.; Sun, Q.; Li, S.; Zhao, S.; Hua, T.; Liu, Z.-J. Structural Basis of CXC Chemokine Receptor 2 Activation and Signalling. *Nature* **2020**, *585*, 135–140. [CrossRef] [PubMed]

15. Shi, X.; Wan, Y.; Wang, N.; Xiang, J.; Wang, T.; Yang, X.; Wang, J.; Dong, X.; Dong, L.; Yan, L.; et al. Selection of a Picomolar Antibody That Targets CXCR2-Mediated Neutrophil Activation and Alleviates EAE Symptoms. *Nat. Commun.* **2021**, *12*, 2547. [CrossRef] [PubMed]
16. Liu, K.; Shen, L.; Wu, M.; Liu, Z.; Hua, T. Structural Insights into the Activation of Chemokine Receptor CXCR2. *FEBS J.* **2022**, *289*, 386–393. [CrossRef]
17. Rose, J.J.; Foley, J.F.; Murphy, P.M.; Venkatesan, S. On the Mechanism and Significance of Ligand-Induced Internalization of Human Neutrophil Chemokine Receptors CXCR1 and CXCR2. *J. Biol. Chem.* **2004**, *279*, 24372–24386. [CrossRef]
18. Prado, G.N.; Suetomi, K.; Shumate, D.; Maxwell, C.; Ravindran, A.; Rajarathnam, K.; Navarro, J. Chemokine Signaling Specificity: Essential Role for the N-Terminal Domain of Chemokine Receptors. *Biochem. USA* **2007**, *46*, 8961–8968. [CrossRef]
19. Manufacture's Information on Ab273068. Available online: https://www.abcam.co.jp/recombinant-human-coronavirus-sars-cov-2-spike-glycoprotein-s1-active-ab273068.html (accessed on 21 February 2022).
20. Yuan, M.; Wu, N.C.; Zhu, X.; Lee, C.-C.D.; So, R.T.Y.; Lv, H.; Mok, C.K.P.; Wilson, I.A. A Highly Conserved Cryptic Epitope in the Receptor Binding Domains of SARS-CoV-2 and SARS-CoV. *Science* **2020**, *368*, 630–633. [CrossRef]
21. Masso-Silva, J.A.; Moshensky, A.; Lam, M.T.Y.; Odish, M.; Patel, A.; Xu, L.; Hansen, E.; Trescott, S.; Nguyen, C.; Kim, R.; et al. Increased Peripheral Blood Neutrophil Activation Phenotypes and NETosis in Critically Ill COVID-19 Patients: A Case Series and Review of the Literature. *Clin. Infect. Dis. Off. Publ. Infect. Dis. Soc. Am.* **2021**, ciab437. [CrossRef]
22. Meizlish, M.L.; Pine, A.B.; Bishai, J.D.; Goshua, G.; Nadelmann, E.R.; Simonov, M.; Chang, C.-H.; Zhang, H.; Shallow, M.; Bahel, P.; et al. A Neutrophil Activation Signature Predicts Critical Illness and Mortality in COVID-19. *Blood Adv.* **2021**, *5*, 1164–1177. [CrossRef] [PubMed]
23. Mukaida, N. Pathophysiological Roles of Interleukin-8/CXCL8 in Pulmonary Diseases. *Am. J. Physiol.-Lung C* **2003**, *284*, L566–L577. [CrossRef] [PubMed]
24. Middleton, J.; Neil, S.; Wintle, J.; Clark-Lewis, I.; Moore, H.; Lam, C.; Auer, M.; Hub, E.; Rot, A. Transcytosis and Surface Presentation of IL-8 by Venular Endothelial Cells. *Cell* **1997**, *91*, 385–395. [CrossRef]
25. Chuntharapai, A.; Kim, K.J. Regulation of the Expression of IL-8 Receptor A/B by IL-8: Possible Functions of Each Receptor. *J. Immunol. Baltim. Md.* **1995**, *155*, 2587–2594.
26. Kledal, T.N.; Rosenkilde, M.M.; Schwartz, T.W. Selective Recognition of the Membrane-bound CX3C Chemokine, Fractalkine, by the Human Cytomegalovirus-encoded Broad-spectrum Receptor US28. *FEBS Lett.* **1998**, *441*, 209–214. [CrossRef]
27. Desmetz, C.; Lin, Y.; Mettling, C.; Portalès, P.; Rabesandratana, H.; Clot, J.; Corbeau, P. The Strength of the Chemotactic Response to a CCR5 Binding Chemokine Is Determined by the Level of Cell Surface CCR5 Density. *Immunology* **2006**, *119*, 551–561. [CrossRef] [PubMed]
28. Camargo, J.F.; Quinones, M.P.; Mummidi, S.; Srinivas, S.; Gaitan, A.A.; Begum, K.; Jimenez, F.; VanCompernolle, S.; Unutmaz, D.; Ahuja, S.S.; et al. CCR5 Expression Levels Influence NFAT Translocation, IL-2 Production, and Subsequent Signaling Events during T Lymphocyte Activation. *J. Immunol.* **2009**, *182*, 171–182. [CrossRef]
29. Bodaghi, B.; Jones, T.R.; Zipeto, D.; Vita, C.; Sun, L.; Laurent, L.; Arenzana-Seisdedos, F.; Virelizier, J.-L.; Michelson, S. Chemokine Sequestration by Viral Chemoreceptors as a Novel Viral Escape Strategy: Withdrawal of Chemokines from the Environment of Cytomegalovirus-Infected Cells. *J. Exp. Med.* **1998**, *188*, 855–866. [CrossRef]
30. Billstrom, M.A.; Lehman, L.A.; Worthen, G.S. Depletion of Extracellular RANTES during Human Cytomegalovirus Infection of Endothelial Cells. *Am. J. Resp. Cell Mol.* **1999**, *21*, 163–167. [CrossRef]
31. Kanduc, D.; Shoenfeld, Y. Molecular Mimicry between SARS-CoV-2 Spike Glycoprotein and Mammalian Proteomes: Implications for the Vaccine. *Immunol. Res.* **2020**, *68*, 1–4. [CrossRef]
32. Beaudoin, C.A.; Jamasb, A.R.; Alsulami, A.F.; Copoiu, L.; van Tonder, A.J.; Hala, S.; Bannerman, B.P.; Thomas, S.E.; Vedithi, S.C.; Torres, P.H.M.; et al. Predicted Structural Mimicry of Spike Receptor-Binding Motifs from Highly Pathogenic Human Coronaviruses. *Comput. Struct. Biotechnol. J.* **2021**, *19*, 3938–3953. [CrossRef] [PubMed]
33. Knight, J.S.; Caricchio, R.; Casanova, J.L.; Combes, A.J.; Diamond, B.; Fox, S.E.; Hanauer, D.A.; James, J.A.; Kanthi, Y.; Ladd, V.; et al. The Intersection of COVID-19 and Autoimmunity. *J. Clin. Investig.* **2021**, *131*. [CrossRef]
34. Cheng, M.H.; Zhang, S.; Porritt, R.A.; Rivas, M.N.; Paschold, L.; Willscher, E.; Binder, M.; Arditi, M.; Bahar, I. Superantigenic Character of an Insert Unique to SARS-CoV-2 Spike Supported by Skewed TCR Repertoire in Patients with Hyperinflammation. *Proc. Natl. Acad. Sci. USA* **2020**, *117*, 25254–25262. [CrossRef]
35. Wucherpfennig, K.W. Mechanisms for the Induction of Autoimmunity by Infectious Agents. *J. Clin. Investig.* **2001**, *108*, 1097–1104. [CrossRef] [PubMed]
36. Segal, Y.; Shoenfeld, Y. Vaccine-Induced Autoimmunity: The Role of Molecular Mimicry and Immune Crossreaction. *Cell Mol. Immunol.* **2018**, *15*, 586–594. [CrossRef] [PubMed]
37. Chang, S.E.; Feng, A.; Meng, W.; Apostolidis, S.A.; Mack, E.; Artandi, M.; Barman, L.; Bennett, K.; Chakraborty, S.; Chang, I.; et al. New-Onset IgG Autoantibodies in Hospitalized Patients with COVID-19. *Nat. Commun.* **2021**, *12*, 5417. [CrossRef]
38. Ishay, Y.; Kenig, A.; Tsemach-Toren, T.; Amer, R.; Rubin, L.; Hershkovitz, Y.; Kharouf, F. Autoimmune Phenomena Following SARS-CoV-2 Vaccination. *Int. Immunopharmacol.* **2021**, *99*, 107970. [CrossRef] [PubMed]
39. Boshuizen, R.S.; Marsden, C.; Turkstra, J.; Rossant, C.J.; Slootstra, J.; Copley, C.; Schwamborn, K. A Combination of in Vitro Techniques for Efficient Discovery of Functional Monoclonal Antibodies against Human CXC Chemokine Receptor-2 (CXCR2). *Mabs* **2014**, *6*, 1415–1424. [CrossRef] [PubMed]

40. Wu, L.; Ruffing, N.; Shi, X.; Newman, W.; Soler, D.; Mackay, C.R.; Qin, S. Discrete Steps in Binding and Signaling of Interleukin-8 with Its Receptor. *J. Biol. Chem.* **1996**, *271*, 31202–31209. [CrossRef] [PubMed]
41. Alam, M.J.; Xie, L.; Ang, C.; Fahimi, F.; Willingham, S.B.; Kueh, A.J.; Herold, M.J.; Mackay, C.R.; Robert, R. Therapeutic Blockade of CXCR2 Rapidly Clears Inflammation in Arthritis and Atopic Dermatitis Models: Demonstration with Surrogate and Humanized Antibodies. *Mabs* **2020**, *12*, 1856460. [CrossRef]
42. *BD FACSAriaTM II & III Cell Sorter Training Manual Ver1.1*; Nippon Becton Dickinson Co., Ltd.: Tokyo, Japan, 2016.